[6] Fidler IJ. Orthotopic implantation of human colon carcinomas into nude mice provides a valuable model for the biology and therapy of metastasis. Cancer Metastasis Rev 1991;10:229. http://dx.doi.org/10.1007/BF00050794.
[7] Couzin-Frankel J. The littlest patient. Science 2014;346:24.
[8] Rashid OM, Nagahashi M, Ramachandran S, et al. An improved syngeneic orthotopic murine model of human breast cancer progression. Breast Cancer Res Treat 2014;147:501. http://dx.doi.org/10.1007/s10549-014-3118-0.
[9] Rashid OM, Nagahashi M, Ramachandran S, et al. Is tail vein injection a relevant breast cancer lung metastasis model? J Thorac Dis 2013;5:385. http://dx.doi.org/10.3978/j.issn.2072-1439.2013.06.17.
[10] Nagahashi M, Ramachandran S, Kim EY, et al. Sphingosine-1-phosphate produced by sphingosine kinase 1 promotes breast cancer progression by stimulating angiogenesis and lymphangiogenesis. Cancer Res 2012;72:726. http://dx.doi.org/10.1158/0008-5472.CAN-11-2167.
[11] Hoffman R. Orthotopic metastatic (MetaMouse) models for discovery and development of novel chemotherapy. Methods Mol Med 2005;111:297.
[12] Rashid OM, Nagahashi M, Ramachandran S, et al. Resection of the primary tumor improves survival in metastatic breast cancer by reducing overall tumor burden. Surgery 2013;153:771. http://dx.doi.org/10.1016/j.surg.2013.02.002.
[13] Narumi K, Udagawa T, Kondoh A, et al. In vivo delivery of interferon-α gene enhances tumor immunity and suppresses immunotolerance in reconstituted lymphopenic hosts. Gene Ther 2012;19:34. http://dx.doi.org/10.1038/gt.2011.73.
[14] Thalheimer A, Otto C, Bueter M, et al. Tumor cell dissemination in a human colon cancer animal model: orthotopic implantation or intraportal injection? Eur J Surg Res 2009;42:195.
[15] Thalheimer A, Korb D, Bönicke L, et al. Noninvasive visualization of tumor growth in a human colorectal liver metastases xenograft model using bioluminescence in vivo imaging. J Surg Res 2013;185:143. http://dx.doi.org/10.1016/j.jss.2013.03.024.
[16] Metildi CA, Kaushal S, Luiken GA, Talamini MA, Hoffman RM, Bouvet M. Fluorescently labeled chimeric anti-CEA antibody improves detection and resection of human colon cancer in a patient-derived orthotopic xenograft (PDOX) nude mouse model. J Surg Oncol 2014;109:451. http://dx.doi.org/10.1002/jso.23507.
[17] Hoffman R. Imageable clinically relevant mouse models of metastasis. Metastasis Res Protoc 2014;1070:141.
[18] Jin H, Yang Z, Wang J, Zhang S, Sun Y, Ding Y. A superficial colon tumor model involving subcutaneous colon translocation and orthotopic transplantation of green fluorescent protein-expressing human colon tumor. Tumour Biol 2011;32:391. http://dx.doi.org/10.1007/s13277-010-0132-7.
[19] Kruse J, von Bernstorff W, Evert K, et al. Macrophages promote tumour growth and liver metastasis in an orthotopic syngeneic mouse model of colon cancer. Int J Colorectal Dis 2013;28:1337. http://dx.doi.org/10.1007/s00384-013-1703-z.
[20] Rajput A, Dominguez San Martin I, Rose R, et al. Characterization of HCT116 human colon cancer cells in an orthotopic model. J Surg Res 2008;147:276. http://dx.doi.org/10.1016/j.jss.2007.04.021.
[21] Yong HJ, Choi Y, Joo HK, et al. Immune response to firefly luciferase as a naked DNA. Cancer Biol Ther 2007;6:781. http://dx.doi.org/10.4161/cbt.6.5.4005.
[22] Su W, Zhou M, Zheng Y, et al. Bioluminescence reporter gene imaging characterize human embryonic stem cell-derived teratoma formation. J Cell Biochem 2011;112:840. http://dx.doi.org/10.1002/jcb.22982.
[23] Hwang JE, Shim HJ, Park YK, et al. Intravenous KITENIN shRNA injection suppresses hepatic metastasis and recurrence of colon cancer in an orthotopic mouse model. J Korean Med Sci 2011;26:1439. http://dx.doi.org/10.3346/jkms.2011.26.11.1439.
[24] Mordant P, Loriot Y, Lahon B, et al. Bioluminescent orthotopic mouse models of human localized non-small cell lung cancer: feasibility and identification of circulating tumour cells. PLoS One 2011;6:10. http://dx.doi.org/10.1371/journal.pone.0026073.
[25] Podetz-Pedersen KM, Vezys V, Somia NV, Russell SJ, McIvor RS. Cellular immune response against firefly luciferase after sleeping beauty-mediated gene transfer in vivo. Hum Gene Ther 2014;25:955. http://dx.doi.org/10.1089/hum.2014.048.
[26] Clark AJ, Safaee M, Oh T, et al. Stable luciferase expression does not alter immunologic or in vivo growth properties of GL261 murine glioma cells. J Transl Med 2014;12:1. http://dx.doi.org/10.1186/s12967-014-0345-4.
[27] Belnap L, Cleveland P. Immunogenicity of chemically induced murine colon cancers. Cancer Res 1979;39:1174.
[28] Kishimoto H, Momiyama M, Aki R, et al. Development of a clinically-precise mouse model of rectal cancer. PLoS One 2013;8:1. http://dx.doi.org/10.1371/journal.pone.0079453.

The Journal of Immunology

# Proinflammatory Proteins S100A8/S100A9 Activate NK Cells via Interaction with RAGE

Kenta Narumi, Reina Miyakawa, Ryosuke Ueda, Hisayoshi Hashimoto, Yuki Yamamoto, Teruhiko Yoshida and Kazunori Aoki



*J Immunol* 2015; 194:5539-5548; Prepublished online 24 April 2015;
doi: 10.4049/jimmunol.1402301
http://www.jimmunol.org/content/194/11/5539



*The Journal of Immunology* is published twice each month by
The American Association of Immunologists, Inc.,
9650 Rockville Pike, Bethesda, MD 20814-3994.

Print ISSN: 0022-1767 Online ISSN: 1550-6606.

# Proinflammatory Proteins S100A8/S100A9 Activate NK Cells via Interaction with RAGE

**Kenta Narumi,* Reina Miyakawa,* Ryosuke Ueda,* Hisayoshi Hashimoto,* Yuki Yamamoto,* Teruhiko Yoshida,† and Kazunori Aoki***

**S100A8/A9, a proinflammatory protein, is upregulated in inflammatory diseases, and also has a tumor-promoting activity by the recruitment of myeloid cells and tumor cell invasion. However, whether the expression of S100A8/A9 in tumors predicts a good or poor prognosis is controversial in the clinical setting. In this study, to clarify the in vivo role of S100A8/A9 in the tumor microenvironment, we s.c. inoculated Pan02 cells stably expressing S100A8 and S100A9 proteins (Pan02-S100A8/A9) in syngeneic C57BL/6 mice. Unexpectedly, after small tumor nodules were once established, they rapidly disappeared. Flow cytometry showed that the number of NK cells in the tumors was increased, and an administration of anti-asialoGM1 Ab for NK cell depletion promoted the growth of Pan02-S100A8/A9 s.c. tumors. Although the S100A8/A9 proteins alone did not change the IFN-γ expression of NK cells in vitro, a coculture with Pan02 cells, which express Rae-1, induced IFN-γ production, and Pan02-S100A8/A9 cells further increased the number of IFN-γ$^+$ NK cells, suggesting that S100A8/A9 enhanced the NK group 2D ligand-mediated intracellular activation pathway in NK cells. We then examined whether NK cell activation by S100A8/A9 was via their binding to receptor of advanced glycation end product (RAGE) by using the inhibitors. RAGE antagonistic peptide and anti-RAGE Ab inhibited the IFN-γ production of NK cells induced by S100A8/A9 proteins, and an administration of FPS-ZM1, a RAGE inhibitor, significantly enhanced the in vivo growth of Pan02-S100A8/A9 tumors. We thus found a novel activation mechanism of NK cells via S100A8/A9–RAGE signaling, which may open a novel perspective on the in vivo interaction between inflammation and innate immunity.**
*The Journal of Immunology*, **2015, 194: 5539–5548.**

Natural killer cells belong to the cellular component of the innate immune systems and have cytotoxic and cytokine-producing capacities, which play a critical role in cancer immune surveillance (1, 2). NK cell activation is regulated by various activating and inhibitory cell surface receptors, which detect nonself ligands or change in the expression of self-molecules on infected or transformed cells (2). NK cells need to be primed with cytokines such as IL-12, IL-15, and IL-18, and by crosstalk with accessory cells to achieve their effector potential (3). Although multiple mechanisms have been clarified for the acquisition of their effector functions (4), it is believed that there are still unknown major mediators for modulating the maturation, activation, and survival of NK cells (4).

S100A8 and S100A9, which belong to a family of 25 homologous low-m.w. intracellular calcium-binding proteins, are constitutively expressed by myeloid cells, including neutrophils, but not by lymphocytes. S100A8/A9 is a proinflammatory heterodimer, and is upregulated in inflammatory diseases such as rheumatoid arthritis and inflammatory bowel disease. In addition, S100A8/A9 protein levels are usually elevated in human primary tumor tissues such as the skin, breast, thyroid, liver, pancreas, and lung cancers (5). A tumor-promoting activity of S100A8/A9 has been demonstrated in various mouse models: S100A8/A9 was essential for the accumulation of myeloid-derived suppressor cells in tumors (6), and it was important in the suppression of dendritic cell function (7). Consistent with these findings, an overexpression of S100A8 and/or S100A9 significantly correlates with tumor progression and worse outcome in the patients with breast cancer, prostate cancer, bladder cancer, and colon cancer (8–12). In contrast, several studies reported that the expression is associated with tumor response to chemotherapy in cervical cancer and also correlates with a good prognosis in gastric and lung cancers (13–16). Therefore, whether an upregulation of S100A8/A9 in tumors predicts a good or poor prognosis in the clinical setting is still controversial.

In this study, to clarify the in vivo role of S100A8 and S100A9 proteins in the tumor microenvironment, S100A8- and/or S100A9-expressing cancer cell lines were inoculated in mice as a model of a human solid cancer. Unexpectedly, the growth of S100A8- and/or S00A9-expressing s.c. tumors was markedly suppressed, which was closely related with the activation of NK cells. We describe in this work a novel immunoregulatory function of S100A8/A9 proteins in the guidance of NK cell activation via their interaction with receptor of advanced glycation end product (RAGE), which is a multiligand receptor for several molecules, including advanced glycation end product, high mobility group box 1, and S100A8/A9 (17).

## Materials and Methods

### *Animals and tumor cell lines*

Seven- to nine-wk-old female C57BL/6 (H-2$^b$), BALB/c (H-2$^d$), and BALB/c nude (H-2$^d$) mice were purchased from Charles River Japan

*Division of Molecular and Cellular Medicine, National Cancer Center Research Institute, Tokyo 104-0045, Japan; and †Division of Genetics, National Cancer Center Research Institute, Tokyo 104-0045, Japan

Received for publication September 12, 2014. Accepted for publication March 29, 2015.

This work was supported in part by a Grant-in-Aid for Third Term Comprehensive 10-Year Strategy for Cancer Control from the Ministry of Health, Labour, and Welfare of Japan, grants-in-aid for research from the Ministry of Health, Labour, and Welfare of Japan, and by the National Cancer Center Research and Development Fund (23-A-38, 23-A-44, and 26-A-11).

Address correspondence and reprint requests to Dr. Kazunori Aoki, Division of Molecular and Cellular Medicine, National Cancer Center Research Institute, 5-1-1 Tsukiji, Chuo-ku, Tokyo 104-0045, Japan. E-mail address: kaoki@ncc.go.jp

The online version of this article contains supplemental material.

Abbreviations used in this article: NKG2D, NK group 2D; RAGE, receptor of advanced glycation end product; RAP, RAGE antagonistic peptide.

 0022-1767/15/$25.00

www.jimmunol.org/cgi/doi/10.4049/jimmunol.1402301

(Kanagawa, Japan). Animal studies were carried out according to the *Guideline for Animal Experiments* of the National Cancer Center Research Institute and approved by the Institutional Committee for Ethics in Animal Experimentation. Pan02 (National Cancer Institute, Frederick, MD) is a C57BL/6-derived pancreatic cancer cell line; CT26 (American Type Culture Collection, Rockville, MD) is a BALB/c-derived colon cancer cell line; and YAC-1 (American Type Culture Collection) is a mouse lymphoma cell line. The cells were maintained in a RPMI 1640 medium containing 10% heat-inactivated FBS (ICN Biomedicals, Irvine, CA), 2 mM L-glutamine, and 0.15% sodium bicarbonate (complete RPMI 1640). The S100A8- and/or S100A9-expressing Pan02 and CT26 cells were generated by retrovirus-mediated transduction of murine S100A8 and S100A9 cDNAs, and designated as Pan02-S100A8, Pan02-S100A9, Pan02-S100A8/A9, CT26-S100A8, CT26-S100A9, and CT26-S100A8/A9 cells, respectively. As a negative control, DsRed-expressing Pan02 and CT26 cells were generated and designated as Pan02-DsRed and CT26-DsRed, respectively. The amounts of S100A8/A9 proteins of cell lysates of Pan02-S100A8/A9, CT26-S100A8/A9 cells, and Gr-1$^+$ neutrophils were 0.95, 1.10, and 1.29 ng per $2 \times 10^6$ cells, respectively, by S100A8/A9 ELISA kit (Immunodiagnostik, Bensheim, Germany).

### *In vitro cell proliferation assay*

Pan02, Pan02-S100A8/A9, CT26, and CT26-S100A8/A9 cells were seeded at $1 \times 10^3$ per well in 96-well plates. The cell numbers were assessed by a colorimetric cell viability assay using a water-soluble tetrazolium salt (Tetracolor One; Seikagaku, Tokyo, Japan) at 24, 48, 72, 96, and 120 h after the cell seeding. Absorbance was determined by spectrophotometry using a wavelength of 450 nm with 600 nm as a reference. The assays (carried out in four wells) were repeated three times.

### *Soft-agar colony formation assay*

A soft-agar colony formation assay of S100A8/A9-expressing cells was performed by using Cytoselect 96-Well Cell Transformation Assay kit (Cell Biolabs, San Diego, CA). We harvested cells in culture medium at $1 \times 10^3$ cells/well, following incubation of the cells for 6 d at 37°C and 5% $CO_2$. We examined the cell colony formation under a light microscope ($n = 3$).

### *RT-PCR analyses of S100A8 and S100A9 expression*

PCR amplification of murine S100A8, S100A9, and β-actin was carried out using total RNA from the S100A8- and/or S100A9-transfected Pan02 and CT26 cells in a 50 μl PCR mixture containing 1.5 mM $MgCl_2$, 0.2 mM dNTPs, 1 U recombinant Taq DNA polymerase, and the following primer sets: S100A8 upstream (5′-TGGTCACTACTGAGTGTCCT-3′) and downstream (5′-CTACTCCTTGTGGCTGTCTT-3′) primers; S100A9 upstream (5′-CCTTCTCAGATGGAGCGCAG-3′) and downstream (5′-TGTCCAGGTCCTCCATGATG-3′) primers; β-actin upstream (5′-CCTCTATGCCAACACAGTGC-3′) and downstream (5′-ATACTCCTGCTTGCTGATCC-3′) primers. In total, 32 cycles (β-actin; 28 cycles) of the PCR were carried out at 95°C for 30 s, 58°C for 30 s, and 72°C for 60 s. The PCR products were electrophoresed on a 1.2% agarose gel.

### *NK cell isolation*

EasySep mouse NK cell enrichment kit (STEMCELL Technologies, Vancouver, BC, Canada) was used according to the manufacturer's instruction. Briefly, single-cell suspension of splenocytes derived from C57BL/6 mice was prepared at a concentration of $1 \times 10^8$ cells/ml complete RPMI 1640 medium, and an EasySep negative selection mixture (50 μl/ml) was added in the cell suspension. After incubation for 15 min, a biotin selection mixture (200 μl/ml) was added and incubated for 10 min. Then magnetic particles (200 μl/ml) were added and incubated for 10 min. Finally, the cell suspension was placed into a magnet for 5 min, and magnetically unlabeled cells were separated and used as NK cells. Flow cytometry showed that ~90% of separated cells were DX5 positive (data not shown).

### *IFN-γ mRNA detection by real-time PCR*

To examine the expression of the IFN-γ mRNA from NK cells cultured with S100A8/A9 proteins, RT-PCR amplification was carried out using total RNA. IFN-γ cDNA was measured by SYBR Green real-time PCR using the Eco Real-Time PCR system (Illumina, San Diego, CA). Briefly, cDNA was added to a final volume of 10 μl/reaction containing 1× SYBR Green PCR Master Mix (Applied Biosystems Japan, Tokyo, Japan) and 100 nM primers IFN-γ sense (5′-TGGCAAAAGGATGGTGACATG-3′) and IFN-γ antisense (5′-TGCTGTTGCTGAAGAAGGTAG-3′), which detected a 149-bp region in IFN-γ cDNA. Thermal cycling conditions were as follows: initial denaturation at 95°C for 10 min, then 55 cycles at 95°C for 10 s and at 60°C for 30 s. Recombinant murine S100A8 and S100A9 proteins were purchased from ProSpec (East Brunswick, NJ). The 2000 U/ml murine rIL-2 (PeproTech, Rocky Hill, NJ) was used to activate NK cells as a positive control. Functional grade purified anti-mouse CD314 (NK group 2D [NKG2D]), purchased from eBioscience (San Diego, CA), is used for in vitro blocking of mouse NKG2D in concentration of 25 μg/ml.

### *Flow cytometry of cell surface marker*

PE-conjugated mouse IFN-γ mAb, FITC-conjugated DX5 (CD49b) mAb, FITC-conjugated mouse H-2K$^b$ mAb, PE-conjugated mouse H-2K$^d$, and allophycocyanin-conjugated CD3 mAb were purchased from BD Pharmingen (San Jose, CA). PE-conjugated mouse CD69 mAb was purchased from eBioscience. PE-conjugated mouse Rae-1 mAb was purchased from R&D Systems (Minneapolis, MN). Cells were analyzed by FACS (FACSCalibur; BD Biosciences, San Jose, CA). A CD3$^-$DX5$^+$ cell population was analyzed as NK cells. Irrelevant IgG mAbs were used as a negative control.

### *Intracellular cytokine staining*

Splenocytes were incubated with S100A8/A9 proteins for 18 h, after which brefeldin A (10 μg/ml) was added for 4 h of incubation. After washing, cells were incubated with the CD3 and DX5 mAbs for 30 min at 4°C, and then fixed and permeabilized with a permeabilization buffer (BD Biosciences). Cells were finally stained with an Ab to IFN-γ for 15 min at room temperature, washed again, and analyzed by FACSCalibur (BD Biosciences). Ten thousand live events were acquired for analysis. Irrelevant IgG mAbs were used as a negative control.

### *ELISPOT assay*

IFN-γ ELISPOT kit (BD Biosciences) was used according to the manufacturer's instructions. Briefly, $2 \times 10^4$ NK cells were cocultured with Pan02 cells in 96-well plates precoated with an anti-mouse IFN-γ Ab (BD Biosciences) for 20 h at 37°C in a complete RPMI 1640 medium in triplicate. After the wells were washed, biotinylated anti-mouse IFN-γ Ab (2 μg/ml) was added and incubated for 2 h at room temperature. A streptavidin–HRP solution was then added and incubated for 1 h at room temperature. After the addition of an aminoethyl carbazole substrate solution, spots were counted under a stereomicroscope. Anti-mouse S100A8 Ab (Millipore) is used for in vitro blocking of mouse S100A8/A9.

### *Cytotoxicity assay*

Target cells (Pan02, Pan02-S100A8/A9, and YAC-1) were labeled with 10 μg/ml 3′,6′-Di(*O*-acetyl)-4′,5′-bis[N,N-bis(carboxymethyl)aminomethyl] fluorescein, tetra-acetoxymethyl ester (calcein-AM; Dojindo Molecular Technologies, Kumamoto, Japan) for a cytotoxicity assay. NK cells and target cells at various ratios were cocultured in the complete RPMI 1640 medium containing 50 U/ml IL-2 in 96-well half-area plates. For the calcein-AM–based Terascan assay, a Terascan instrument (Minerva Tech, Tokyo, Japan) measured the fluorescence emitted by intact target cells. Percent cytotoxicity of the assay was calculated by the following formula: % cytotoxicity = (1 − [(average fluorescence of the sample wells − average fluorescence of the maximal release control wells)/(average fluorescence of the minimal release control wells − average fluorescence of the maximal release control wells)]) × 100.

### *Statistical analysis*

Comparative analyses of the data were performed by the Student $t$ test, using SPSS statistical software (SPSS Japan, Tokyo, Japan). A $p$ value $<0.05$ was considered as a significant difference.

## Results

### *The expression of S100A8 and S100A9 suppressed tumor growth*

First, we examined whether S100A8/A9 were released from Pan02-S100A8/A9 cells. ELISA detected S100A8/A9 protein (1.17 ng/ml) in the culture media of Pan02-S100A8/A9, but not in Pan02 (<0.25 ng/ml). Flow cytometry did not show the expression of S100A8/A9 on the surface of Pan02-S100A8/A9 cells (data not shown). To investigate whether human pancreatic cancer actually expresses S100A8 and S100A9, RT-PCR analysis was performed

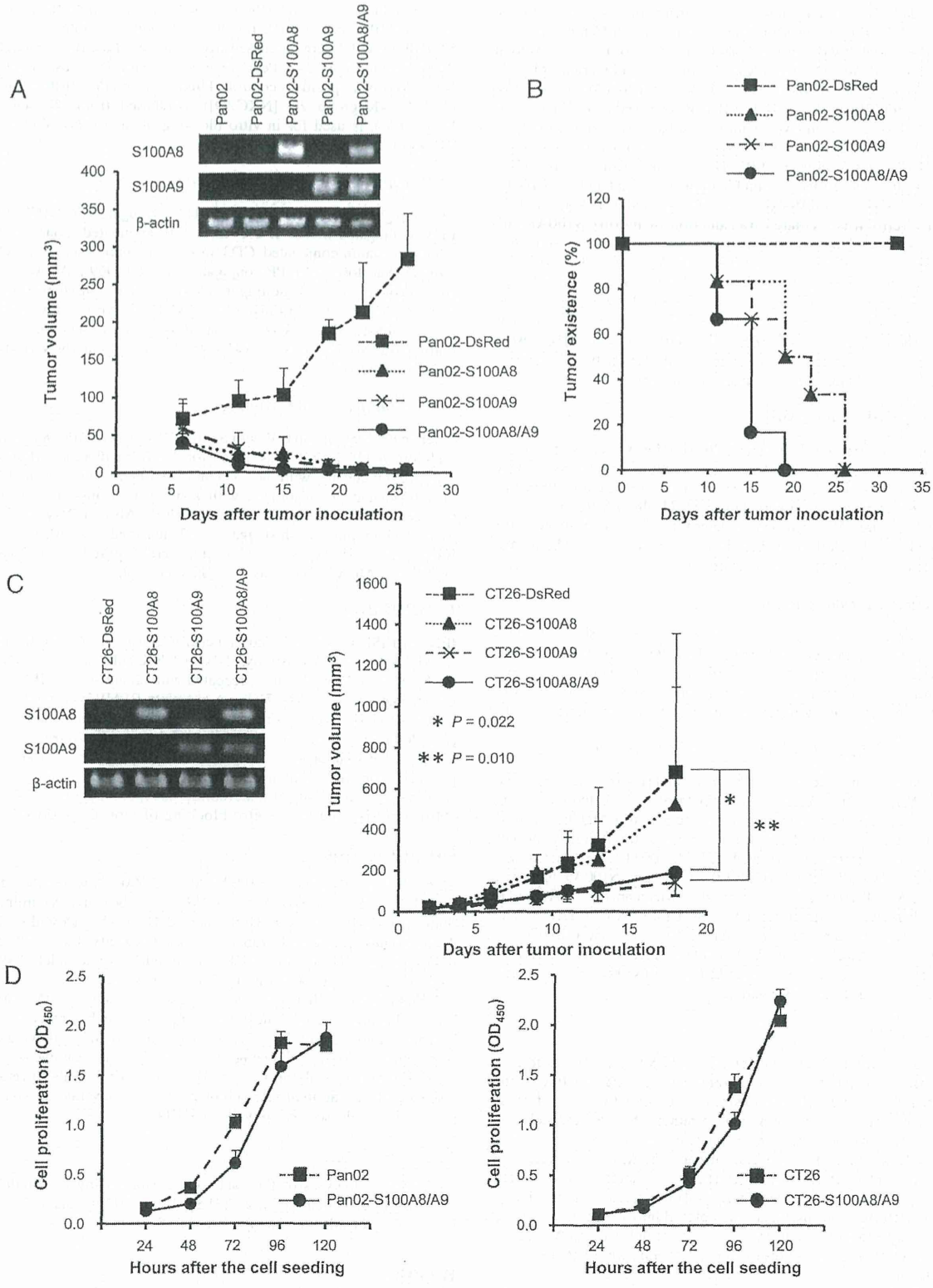


**FIGURE 1.** Growth of S100A8- and S100A9-expressing tumor cells was suppressed in immune-competent mice. (**A**) Rejection of S100A8- and S100A9-expressing Pan02 cells. The expression of S100A8 and S100A9 genes was confirmed in Pan02-S100A8, Pan02-S100A9, and Pan02-S100A8/A9 cells by RT-PCR. The $2 \times 10^6$ of each cell line was s.c. inoculated into the C57BL/6 mice, and the tumor volume was measured at the indicated days after the tumor inoculation ($n = 7$). (**B**) Tumor existence of each s.c. tumor. The tumor existence rate was plotted in the mice of (A). (**C**) Growth suppression of S100A8- and S100A9-expressing CT26 cells. The expression of S100A8 and S100A9 genes was confirmed in CT26-S100A8, CT26-S100A9, and CT26-S100A8/A9 cells by RT-PCR. The $1 \times 10^6$ of each cell line was inoculated s.c. into the BALB/c mice, and the tumor volume was measured at the indicated days ($n = 7$). (**D**) In vitro cell proliferation. The in vitro cell growths of S100A8- and S100A9-expressing Pan02 (*left panel*) and CT26 cells (*right panel*) were measured on the indicated days.

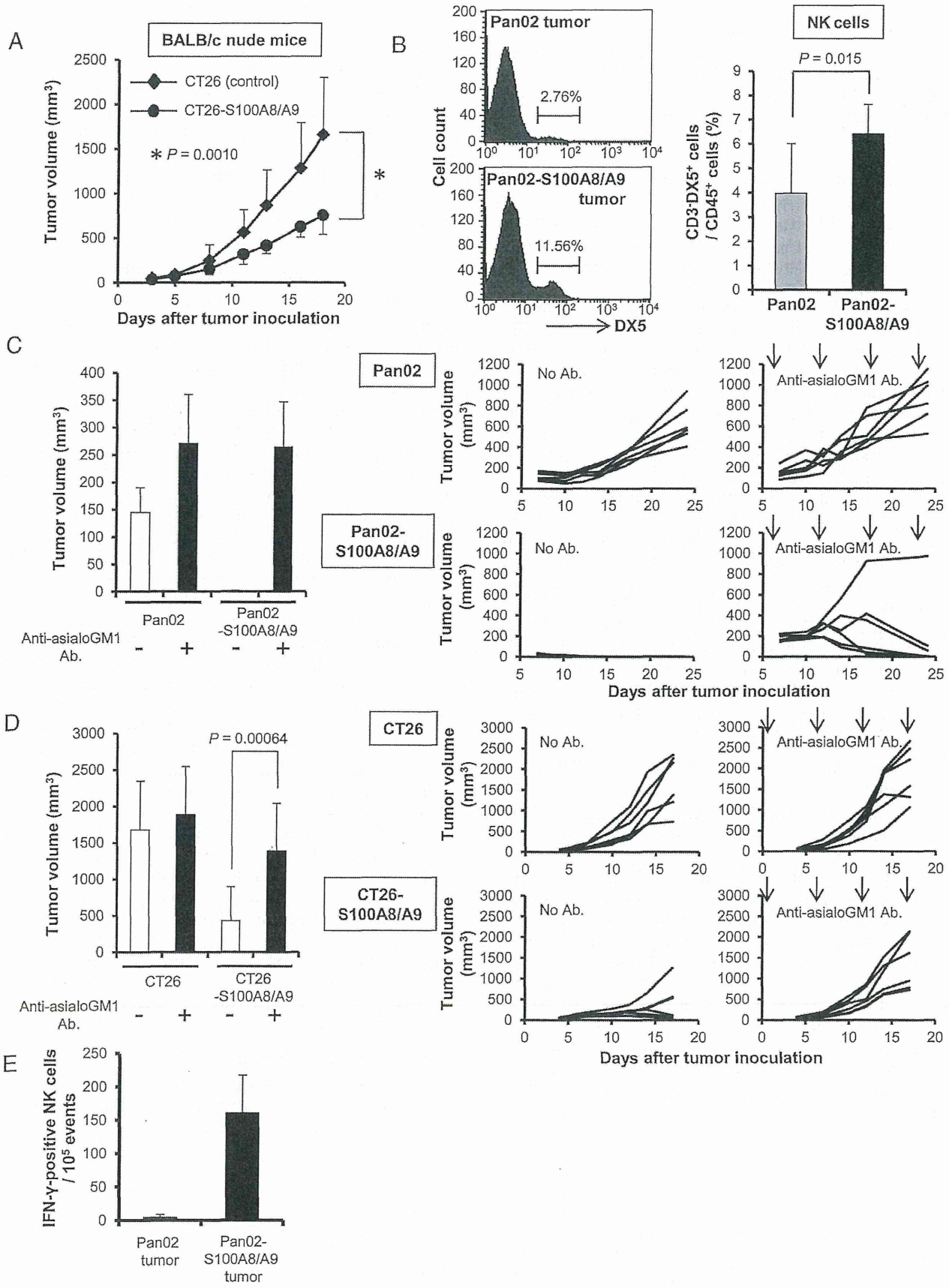


**FIGURE 2.** NK cells attributed to the tumor growth inhibition of S100A8/A9-expressing s.c. tumors. (**A**) The growth suppression of CT26-S100A8/A9 s.c. tumors in the nude mice. A total of $1 \times 10^6$ CT26-S100A8/A9 cells was inoculated into the BALB/c nude mice, and the tumor volume was measured in the indicated days ($n = 7$). (**B**) Percentage of tumor-infiltrating NK cells in Pan02-S100A8/A9 s.c. tumors. Tumors were har- (*Figure legend continues*)

in seven human pancreatic cancer cell lines and human pancreatic epithelial cells. The analysis showed that these cell lines expressed S100A8 and/or S100A9, except for MIA PaCa-2 and human pancreatic epithelial, and KLM-1 and PSN-1 expressed both S100A8 and S100A9 (Supplemental Fig. 1). The concentration of S100A8/A9 was 0.58 ng/ml in the culture media of KLM-1 and 0.33 ng/ml in PSN-1 cells by ELISA, which made little difference from that of Pan02-S100A8/A9.

Then, to investigate the in vivo roles of S100A8 and S100A9 proteins in a tumor microenvironment, Pan02-S100A8, Pan02-S100A9, and Pan02-S100A8/A9 cells were inoculated in syngeneic C57BL/6 mice. Unexpectedly, once small s.c. tumors were established, they rapidly diminished, and then completely disappeared by 19 d after the inoculation (Fig. 1A). The s.c. tumors of Pan02-S100A8/A9 cells were more rapidly rejected as compared with those of Pan02-S100A8 or Pan02-S100A9 cells (Fig. 1B). Then, to confirm that the tumor-suppressive effect was not specific phenomenon for Pan02, S100A8- and S100A9-expressing CT26 cells were inoculated into the syngeneic BALB/c mice. The growth of CT26-S100A8 tumors was unchanged compared with the control CT26-DsRed tumors, whereas CT26-S100A9 and CT26-S100A8/A9 tumors were significantly suppressed when compared with the CT26-DsRed tumors (Fig. 1C). The in vitro cell growth of Pan02-S100A8/A9 and CT26-S100A8/A9 was no different from that of parental Pan02 and CT26 cells, except for Pan02-S100A8/A9 cells at 72 h (Fig. 1D). A soft-agar colony formation assay for 6 d did not show any difference in the number of colonies between S100A8/A9-expressing cells and the parental cells (Pan02: 337.3 ± 56.7 versus Pan02-S100A8/A9: 319.0 ± 31.7, $p = 0.65$, and CT26: 372.3 ± 16.3 versus CT26-S100A8/A9: 380.3 ± 38.7, $p = 0.76$), indicating that the growth of Pan02-S100A8/A9 and CT26-S100A8/A9 was almost the same as that of parental cell lines. These results indicated that an upregulation of S100A8/A9 in cancer cells markedly suppressed the tumor growth in the immune-competent mice.

### *NK cells were responsible for S100A8/A9-mediated tumor growth suppression*

Next, to examine whether $CD4^+$ and $CD8^+$ T cells were associated with the growth suppression of S100A8/A9-expressing tumors, we inoculated CT26-S100A8/A9 cells in the immunodeficient BALB/c nude mice. The growth of CT26-S100A8/A9 s.c. tumors was significantly suppressed in the mice, suggesting that the suppression was caused by NK cells (Fig. 2A). Flow cytometry showed that the number of NK cells infiltrated into the CT26-S100A8/A9 and Pan02-S100A8/A9 tumors was markedly increased as compared with that in the CT26 tumors in BALB/c (Supplemental Fig. 2) and Pan02 tumors in C57BL/6 mice (Fig. 2B), respectively. To confirm that the NK cells were responsible for the growth suppression of S100A8/A9-expressing tumors, we inoculated Pan02-S100A8/A9 cells in C57BL/6 mice, followed by an i.p. injection of anti-asialoGM1 Ab (Wako Chemicals USA, Richmond, VA) to deplete NK cells in vivo. Flow cytometry showed that ~90% of NK cells were depleted in the Ab-treated mice in vivo (data not shown). Pan02-S100A8/A9 tumors in the anti-asialoGM1 Ab–treated mice were significantly larger than those in mice with no Ab treatment, and the tumor size was almost the same as that of the Pan02 tumors treated with Ab (Fig. 2C). In CT26-S100A8/A9 models also, the NK cell depletion significantly increased the growth of S100A8/A9-expressing tumors at day 12 (Fig. 2D). Intracellular cytokine staining showed that a large number of IFN-$\gamma^+$ NK cells was detected in Pan02-S100A8/A9 compared with Pan02 tumors, indicating that NK cells were at an activated state in the Pan02-S100A8/A9 tumors (Fig. 2E). These findings indicated that the growth suppression of S100A8/A9-expressing tumors was closely dependent on NK cells.

### *S100A8/A9-expressing cancer cells activated NK cells*

To examine whether S100A8/A9 proteins directly enhanced a cytotoxic activity of NK cells, $DX5^+$ NK cells were isolated from splenocytes by using magnetic beads–cell sorting, and were cultured in the complete RPMI 1640 medium containing recombinant S100A8 and S100A9 proteins. However, flow cytometry (data not shown) and a sensitive quantitative RT-PCR (Fig. 3A) showed that IFN-γ expression was not upregulated in NK cells cultured with S100A8 and S100A9 proteins. Therefore, we speculated that an additional stimulus was necessary for the S100A8/A9-mediated enhancement of NK cell activity.

We next cultured NK cells with Pan02 and Pan02-S100A8/A9 cells and assessed IFN-γ production from the NK cells. On the Pan02 cells, the expression of MHC class-I molecule ($H\text{-}2K^b$) was considerably low, and Rae-1, one of the NKG2D ligands, was markedly expressed in the in vitro culture condition (Fig. 3B). Expression level of Rae-1 protein on Pan02-S100A8, Pan02-S100A9, and Pan02-S100A8/A9 was almost the same as Pan02 (Supplemental Fig. 3). ELISPOT assay showed that the coculture with parental Pan02 cells increased the number of IFN-$\gamma^+$ spots, whereas the Pan02-S100A8/A9 cells induced more IFN-γ production from NK cells than the Pan02 cells did (Fig. 3C). In addition, an in vitro cytotoxic assay showed that NK cells induced cell death in Pan02-S100A8/A9 cells more effectively than in Pan02 cells (Fig. 3D). Then we examined whether the Pan02-S100A8/A9-increased IFN-γ expression could be blocked by S100A8-specific blocking Ab. ELISPOT assay showed that treatment with S100A8 Ab significantly decreased the number of IFN-$\gamma^+$ NK cells cocultured with Pan02-S100A8/A9, but not with Pan02 cells (Fig. 3E), indicating that S100A8/A9 protein is certainly associated with the Pan02-S100A8/A9-mediated activation of NK cells. Furthermore, production of IFN-γ from NK cells induced by Pan02-S100A8/A9 was decreased by the addition of NKG2D neutralizing Ab (Fig. 3F, 3G). These findings indicated that S100A8/A9 enhanced the NKG2D ligand-mediated activity pathway in NK cells.

### *S100A8/A9 activated NK cells through RAGE*

It is known that S100A8/A9 binds to RAGE and TLR4 (18, 19). Our flow cytometry data indicated that murine NK cells expressed RAGE, but not TLR4, on their surface (Fig. 4A). To clarify that

vested at 10 d after tumor inoculation and processed into single-cell suspension, and the percentage of $DX5^+$ cells was analyzed by flow cytometry ($n = 3$). (**C**) Growth of Pan02-S100A8/A9 tumors in NK cell–depleted mice. Pan02-S100A8/A9 cells were inoculated in the C57BL/c mice, and 0.5 mg anti-asialoGM1 Ab was i.p. injected in the mice at 2 d after the tumor inoculation. The injection was repeated every 5–6 d throughout the entire experimental period. The tumor volume was measured at the indicated days ($n = 7$) (*right panel*). Tumor volumes at 12 d after tumor inoculation are presented (*left panel*). (**D**) Growth of CT26-S100A8/A9 tumors in NK cell–depleted mice. CT26-S100A8/A9 cells were inoculated into the BALB/c mice, and 0.5 mg anti-asialoGM1 Ab was i.p. injected into the mice every 5–6 d from 2 d after the tumor inoculation ($n = 7$) (*right panel*). Tumor volumes at 12 d after tumor inoculation are presented (*left panel*). (**E**) IFN-$\gamma^+$ NK cells in Pan02-S100A8/A9 tumors. Tumor-infiltrating cells were cultured for 4 h with brefeldin A (10 μg/ml) and murine rIL-2 (100 U/ml). The number of $CD3^-DX5^+$IFN-$\gamma^+$NK cells per $10^5$ events was plotted ($n = 6$).

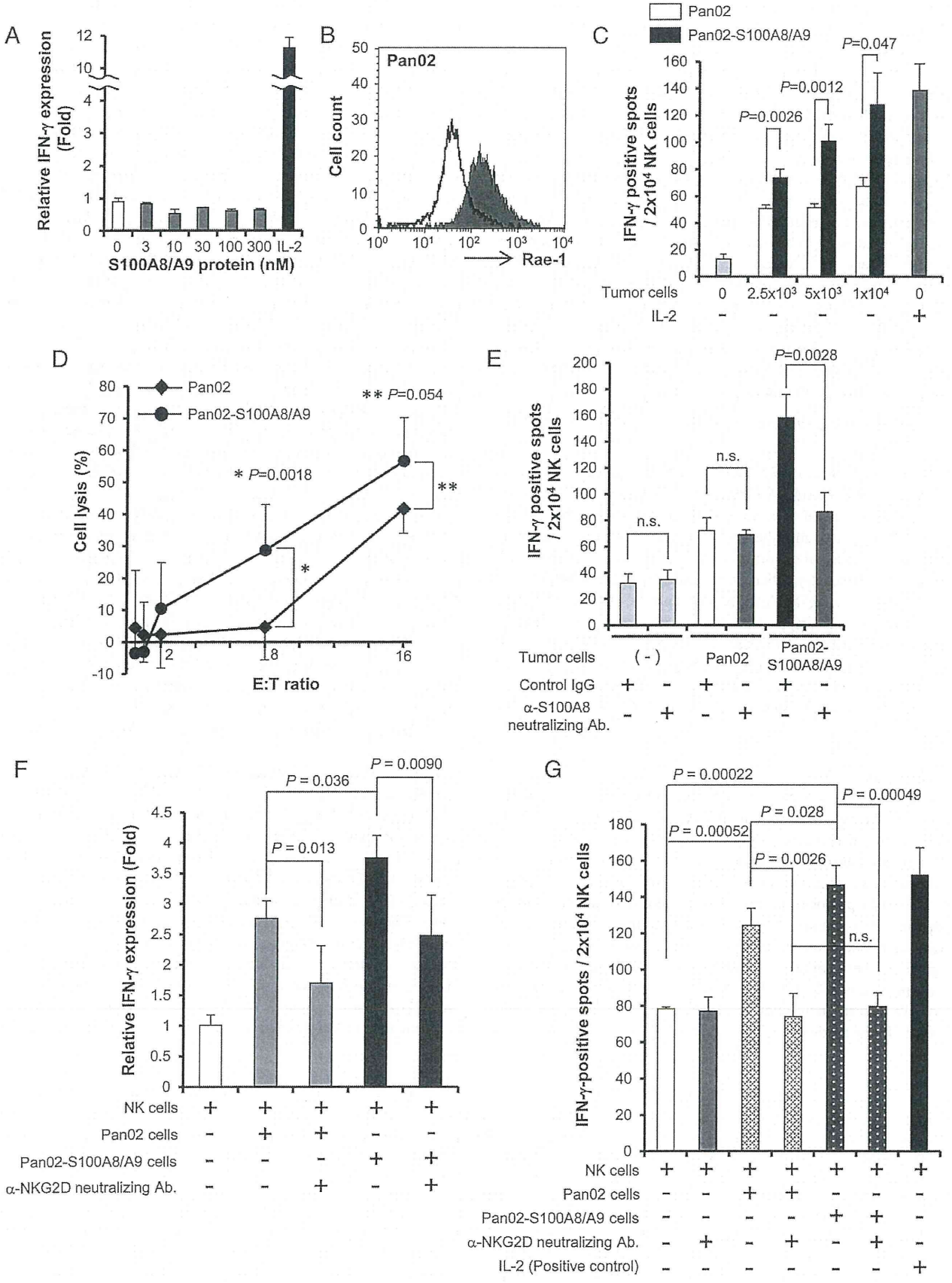


**FIGURE 3.** S100A8/A9 enhanced the cytotoxicity of NK cells for Pan02-S100A8/A9 cells. (**A**) IFN-γ expression of NK cells in the in vitro culture with S100A8/A9 proteins. The $CD3^{-}DX5^{+}$ NK cells were isolated from splenocytes and cultured in the complete RPMI 1640 medium containing recombinant S100A8 and S100A9 proteins for 5 h. IFN-γ expression in NK cells was analyzed by real-time PCR ($n = 3$). (**B**) Rae-1 expression on Pan02 cells. Rae-1 expression was examined by flow cytometry in the in vitro culture condition. Filled plot: stained by Rae-1 mAb. Open plot: (*Figure legend continues*)

S100A8/A9-mediated NK cell activation is due to the interaction of S100A8/A9 with RAGE, we used three kinds of RAGE blocker: RAGE antagonistic peptide (RAP) (20), FPS-ZM1 (21), and anti-RAGE Ab. The addition of 2 μM RAP, 230 nM FPS-ZM1, and anti-RAGE Ab did not affect IFN-γ production of NK cells in the absence of S100A8/A9 (Fig. 4B). An IFN-γ ELISPOT assay showed that the coculture with Pan02-S100A8/A9 cells increased IFN-γ expression of NK cells (Fig. 3C), whereas an addition of RAP and FPS-ZM1 into the culture medium decreased the number of IFN-γ spots induced by Pan02-S100A8/A9 cells to the same level that Pan02 cells did (Fig. 4B). IFN-γ production of NK cells was increased in the coculture with Pan02 cells by the addition of S100A8 and S100A9 proteins in a dose-dependent manner, whereas this increase was almost canceled by RAP, FPS-ZM1, and anti-RAGE Ab (Fig. 4C). Moreover, an addition of S100A8/A9 increased NK cell killing for YAC-1 cells in vitro, and this enhanced cytotoxic activity was significantly decreased by treatment with RAP (Fig. 4D). These results indicated that S100A8/A9 activated NK cells via the interaction with RAGE.

*Blockade of RAGE signaling formed Pan02-S100A8/A9 tumors in the mice*

To examine the role of S100A8/A9–RAGE signaling in the rejection of Pan02-S100A8/A9 cells in the C57BL/6 mice, FPS-ZM1 was i.p. administered at a dose of 1 mg/kg every other day in Pan02-S100A8/A9 tumor-bearing C57BL/6 mice. The administration did not affect the growth of Pan02 s.c. tumors (Fig. 5A, *left*), whereas it significantly enhanced the growth of Pan02-S100A8/A9 tumors (Fig. 5A, *right*). Although all Pan02-S100A8/A9 tumors finally disappeared in the absence of FPS-ZM1, tumor masses were formed in half of the cases of Pan02-S100A8/A9 inoculation by RAGE inhibitor (Fig. 5B, Supplemental Fig. 4). These findings indicated that S100A8/A9–RAGE signaling in NK cells was essential in suppressing the growth of S100A8/A9-expressing tumors.

## Discussion

Neutrophils, which occupy 50–70% of WBCs in the peripheral blood, are recruited rapidly to peripheral damage sites, with a primary role in resistance against extracellular pathogens and in acute inflammation (22). Neutrophils constitute the majority of infiltrating cells in acute inflammatory tissues and work as phagocytes and in pathogen killing (23). In addition, numerous other functions are currently attributed to neutrophils, such as the capacity to regulate various aspects of the inflammatory, immune, angiogenic, hematopoietic, wound-healing, antiviral, and antitumoral responses (24, 25). Recent evidence indicated that there is crosstalk between neutrophils and NK cells as follows: NK cell–derived IFN-γ modulates the survival, migration into inflammatory sites, and functional responses of neutrophils, and conversely, neutrophil-derived IL-15 and IL-18 are essential for NK cell activation and proliferation (4). Based on recent observation, it is possible to speculate that additional neutrophil-derived factors affect the activity of NK cells (26). Because in vivo major sources of S100A8/A9 are myeloid cells, including neutrophils (27), this study suggests that neutrophils give a significant signal to NK cells by secreting S100A8/A9 proteins in the presence of NKG2D stimulus, following NK cell activation. Alternatively, there is a possibility that a direct interaction between tumor cells and NK cells is more important for activation than neutrophils, because tumor cells are able to give a dual stimulus of NKG2D ligand-NKG2D and S100A8/A9-RAGE to NK cells at the same time in the same place. To examine the role of neutrophils, we are investigating the relationship between neutrophil-derived S100A8/A9 and activation of NK cells as a next study.

Pan02-S100A8/A9 tumors were rapidly rejected (Fig. 2C), whereas the growth of CT26-S100A8/A9 tumors was suppressed, but not completely rejected in the syngeneic mice (Fig. 2D). NK cells express a repertoire of inhibitory receptors that regulate their activation, and some inhibitory NK receptors are specific for MHC class I (28). Because the expression of MHC class I molecules is diminished on Pan02 cells, whereas CT26 cells express MHC-class I molecules (data not shown), NK cells may result in a stronger antitumor effect in Pan02 tumors as compared with CT26 tumors. Even in asialoGM1 Ab–treated mice, five of six Pan02-S100A8/A9 tumors were rejected at a late phase (Fig. 2C). The immunohistochemistry showed that the numbers of $CD4^+$ and $CD8^+$ T cells infiltrated in Pan02-S100A8/A9 and CT26-S100A8/A9 tumors were significantly increased in Ab-treated mice, which seem to be effectors (data not shown). Therefore, the NK cells may be associated with the tumor growth suppression at early phase after tumor inoculation. The antitumor effect of cellular immunity at a late phase may be dependent on tumor types, which possibly affected tumor growth in the situation of NK cell depletion.

This study showed that the S100A8/A9 proteins alone did not directly activate NK cells in vitro (Fig. 3A), whereas the Pan02 cells stimulated NK cells to produce IFN-γ, and S100A8/A9-expressing Pan02 cells markedly increased IFN-γ production from NK cells (Fig. 3C). Pan02 cells expressed Rae-1, one of the mouse NKG2D ligands, which is reported to activate NK cells via NKG2D (28). Although mouse and human NK cells express numerous activating or coactivating NK receptors, many induce common signaling pathways and thus behave in a similar way: there are mainly three distinct signaling pathways, including the ITAM-bearing NK receptor complexes, the DAP10-associated NKG2D receptor complex, and the CD244 receptor system (29). In particular, ITAM-mediated signaling in NK cells triggers the

stained by isotype control mAb. (**C**) Enhancement of IFN-γ production in NK cells by the coculture with Pan02-S100A8/A9 cells. A total of $2 \times 10^4$ of NK cells was cultured with various numbers of Pan02 or Pan02-S100A8/A9 cells on 96-well plates, and $IFN\text{-}\gamma^+$ spots were measured by the ELISPOT assay ($n = 3$). (**D**) NK cell–killing assay for Pan02 or Pan02-S100A8/A9. Target cells (Pan02 or Pan02-S100A8/A9) were labeled with 10 μg/ml calcein-AM, and $1 \times 10^4$ labeled cells/well were added into 96-well plates. NK cells isolated from C57BL/6 mice were added to the wells at indicated E:T ratios and incubated for 4 h with 50 U/ml murine IL-2 ($n = 3$). Cell lysis was calculated by the calcein-AM–based Terascan assay. (**E**) Number of $IFN\text{-}\gamma^+$ NK cells induced by Pan02-S100A8/A9 was decreased by the addition of S100A8-neutralizing Ab. A total of $2 \times 10^4$ NK cells was cultured with $1 \times 10^4$ Pan02 or Pan02-S100A8/A9 cells on 96-well plates, and $IFN\text{-}\gamma^+$ spots were measured by the ELISPOT assay ($n = 3$). (**F**) Production of IFN-γ from NK cells induced by Pan02-S100A8/A9 was decreased by the addition of NKG2D-neutralizing Ab. A total of $2 \times 10^5$ NK cells and $1 \times 10^4$ Pan02 or Pan02-S100A8/A9 was cocultured in the 96-well plates for 4 h. Anti-mouse NKG2D neutralizing Ab was added at a concentration of 25 μg/ml into the well. IFN-γ expression in NK cells was analyzed by real-time PCR ($n = 4$). (**G**) Number of $IFN\text{-}\gamma^+$ NK cells induced by Pan02-S100A8/A9 was decreased by the addition of NKG2D-neutralizing Ab. A total of $2 \times 10^4$ NK cells was cultured with $1 \times 10^4$ Pan02 or Pan02-S100A8/A9 cells on 96-well plates containing 25 μg/ml NKG2D-neutralizing Ab, and $IFN\text{-}\gamma^+$ spots were measured by the ELISPOT assay ($n = 3$). A total of 2000 U/ml murine rIL-2 was used to activate NK cells as a positive control.

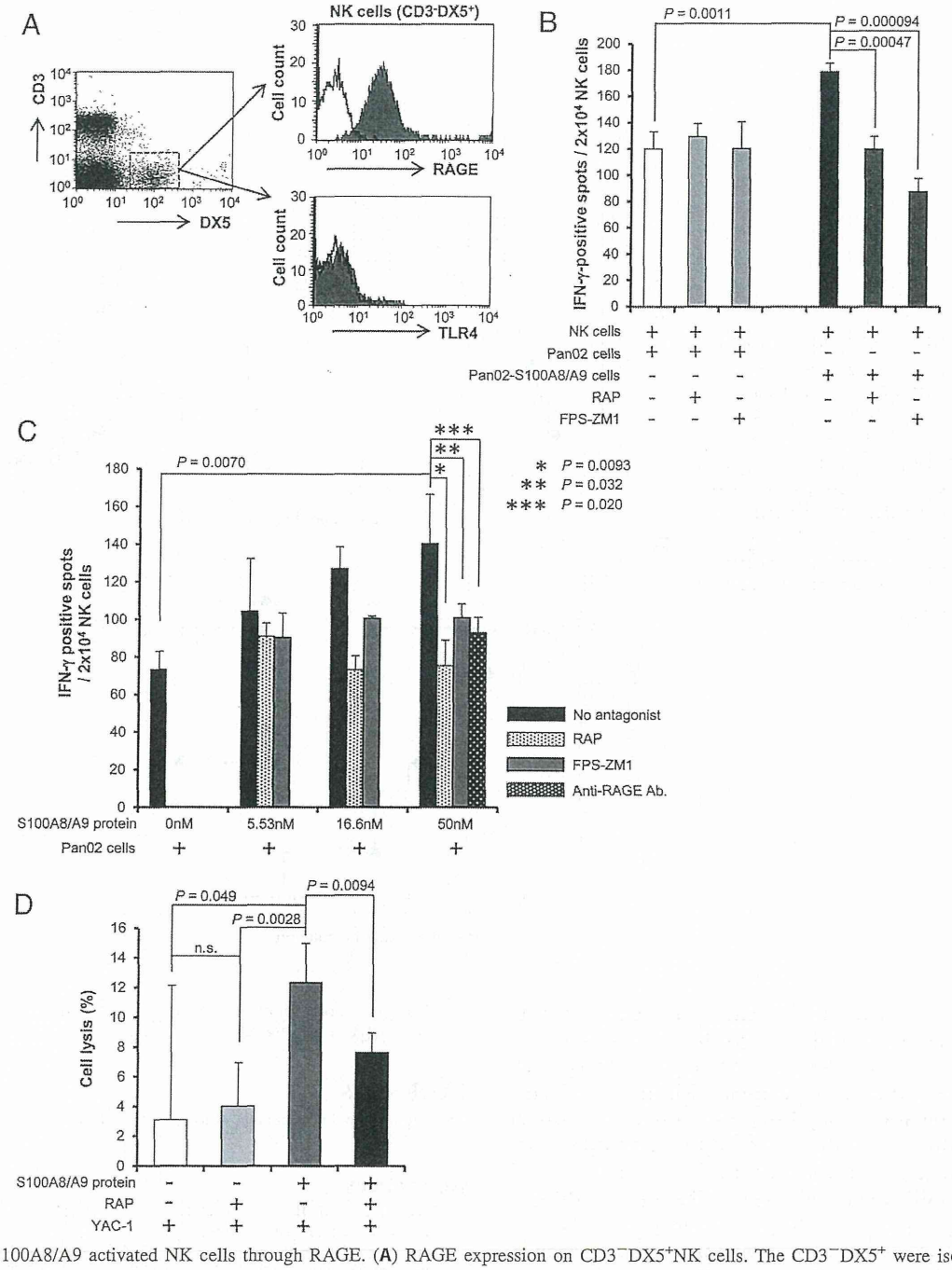


**FIGURE 4.** S100A8/A9 activated NK cells through RAGE. (**A**) RAGE expression on $CD3^{-}DX5^{+}$NK cells. The $CD3^{-}DX5^{+}$ were isolated from the spleen, and the expressions of RAGE and TLR4 were examined by flow cytometry. (**B**) IFN-γ production of NK cells by Pan02-S100A8/A9 cells in the presence of RAP or FPS-ZM1. NK cells were cocultured with Pan02-S100A8/A9 cells in the medium containing RAP (2 μM) or FPS-ZM1 (230 nM), and the number of IFN-$\gamma^{+}$ spots was measured by ELISPOT assay ($n = 3$). (**C**) IFN-γ production of NK cells cocultured with Pan02 cells and S100A8/A9 proteins in the presence of RAGE inhibitors. A total of $2 \times 10^4$ NK and $1 \times 10^4$ Pan02 cells was cocultured in the medium containing recombinant S100A8 and S100A9 proteins at the indicated dose. To investigate RAGE interaction, three RAGE inhibitors, RAP (2 μM), FPS-ZM1 (230 nM), and anti-RAGE Ab (8 μg/ml), were added in the medium. Twenty hours later, the number of IFN-$\gamma^{+}$ spots was examined by ELISPOT assay ($n = 3$). (**D**) NK cell–killing assay in the presence of RAP. YAC-1 cells were labeled with calcein-AM as target cells. YAC-1 cells and NK cells were cocultured with the labeled YAC-1 cells (E:T ratio = 1:2) in the medium containing 5 nM recombinant S100A8/A9 proteins and 50 U/ml murine IL-2 ($n = 3$). YAC-1 cell killing was analyzed by Terascan assay.

activation and translocation of NF-κB and JNK transcription factors (29). In contrast, after binding the ligands to RAGE, several intracellular signalings, such as Jak/Stat, NADPH oxidase, and mitogenactivated protein kinase, brings to NF-κB (30, 31), which enhances the transcription of inflammation-related proteins such as IL-1α, IL-6, TNF-α, and RAGE itself (32). Therefore, S100A8/A9–RAGE signaling may enhance or tune the intracellular signaling pathway of NK cell activation by NKG2D ligands.

S100A8/A9 enhances the NK cell activation, as shown in this study, which acts on tumor suppression. In contrast, several reports indicated that RAGE signaling sustains inflammation and promotes tumor development (6). Hiratsuka et al. (33) reported that